

## Modeling of the Fe-Al phase diagram

D. A. Contreras-Solorio, F. Mejía-Lira, and J. L. Morán-López

*Instituto de Física, Universidad Autónoma de San Luis Potosí, 78000 San Luis Potosí, S.L.P., Mexico*

J. M. Sanchez

*Henry Krumb School of Mines, Columbia University, New York, New York 10027*

(Received 27 June 1988)

The thermodynamic models used to describe the Fe-Al phase diagram are studied in detail. We calculate the phase diagram of Fe-Al within the Bragg-Williams approximation and the tetrahedron approximation of the cluster-variation method, including nearest- and next-nearest-neighbor chemical and magnetic interactions. In contrast to previous calculations performed within the Bragg-Williams approximation, we find that the model does not reproduce the experimentally observed two-phase equilibrium region between a disordered Fe-Al solid solution and a paramagnetic  $B2$  ordered phase. Within the model, the previously reported two-phase coexistence corresponds to metastable equilibrium. The equilibrium phase in that region of the phase diagram is a ferromagnetic  $B2$  phase.

### I. INTRODUCTION

The Fe-Al system is widely regarded, for both experimental and theoretical purposes, as the prototype binary magnetic alloy based on a bcc structure. Consequently, Fe-Al has been the subject of several experimental and theoretical investigations. The experimental work<sup>1,2</sup> has revealed a complex phase diagram topology with phases of different symmetry ( $A2$ ,  $B2$ , and  $DO_3$ ) appearing in both the paramagnetic and ferromagnetic states. Furthermore, the existing experimental evidence<sup>3</sup> indicates a complex low-temperature magnetic behavior near 30 at. % Al. In this region, as the temperature is lowered, the alloy transforms from a paramagnetic to a ferromagnetic phase, reverts to a paramagnetic phase and, finally, it transforms into a spin glass phase.

Much of the theoretical work to date has been aimed at reproducing the Fe-rich portion of the equilibrium phase diagram. These studies are generally based on Bragg-Williams (BW) treatments<sup>4-6</sup> of the free energy, with the exception of the work of Golosov *et al.*<sup>7</sup> who applied the cluster variation method (CVM). These authors, however, neglected magnetism in their CVM modelling of the Fe-Al system. General studies of bcc magnetic alloys with one magnetic component, although not specifically aimed at reproducing the Fe-Al phase diagram, have also been carried out.<sup>8,9</sup> Dünweg and Binder<sup>8</sup> performed a comparative study for model bcc alloys with one magnetic component using Monte Carlo (MC) simulations, the CVM and the BW approximation. These authors found that, whereas the MC and CVM approximations are in close agreement with each other, the phase diagram predicted by the BW approximation was significantly different. In view of such results, we reexamine here the thermodynamic models used to describe the Fe-Al system. The set of interaction parameters used to reproduce the Fe-Al phase diagram by previous authors in the BW approximation are used with the tetrahedron approxima-

tion of the CVM. The more reliable configurational entropy provided by the CVM should give an exacting test of the interactions proposed in the past. As discussed below, we focus also on qualitative differences between the CVM and BW approximation.

Several well-documented features of the Fe-Al phase diagram have been discussed extensively in the literature.<sup>1,2,4-6</sup> In particular there is evidence<sup>1,2</sup> of a two-phase region where a disordered Fe-Al solid solution coexists with a paramagnetic ordered phase with the  $B2$  structure. This two-phase region joins with a line of second-order transitions between the paramagnetic bcc solid solution and the paramagnetic  $B2$  phase in a characteristic tricritical point. The implications of the tricritical point for the possible decomposition modes of Fe-rich Fe-Al alloys have been discussed in detail by Allen and Cahn.<sup>10,11</sup> To the authors best knowledge, there are, at present, three calculations that appear to reproduce this two-phase region: a BW calculation by Sagane and Oki<sup>4</sup> involving first- and second-neighbor magnetic interactions; a calculation involving up to third-neighbor chemical interactions for a nonmagnetic alloy by Hasaka<sup>5</sup>; and a calculation by Semenovskaya<sup>6</sup> that includes chemical and magnetic interactions for a spin 1 model. All these calculations were carried out in the mean-field approximation, although the model developed by Semenovskaya does not treat the chemical and magnetic entropy in the same footing.

As pointed out by Allen and Cahn,<sup>11</sup> magnetic interactions are not needed in order to reproduce a tricritical point, a fact that was confirmed by Hasaka's computation<sup>5</sup> in the BW approximation. Different results are found by Sagane and Oki<sup>4</sup> and by Semenovskaya,<sup>6</sup> who indicate that the two-phase region is between a ferromagnetic disordered phase and the paramagnetic  $B2$  phase, ending at an apparent bicritical point. A motivation for the present work was the fact that several CVM calculations performed by the authors, using a wide range of

first- and second-neighbor chemical and magnetic interactions, failed to reproduce the two-phase region between the bcc disordered ferromagnetic solid solution,  $A2(F)$ , and the paramagnetic ordered phase,  $B2(P)$  reported by Sagane and Oki<sup>4</sup> and by Semenovskaya.<sup>6</sup> We found that the two-phase region between  $A2(F)$  and  $B2(P)$  corresponds to *metastable equilibrium*. In fact, the equilibrium phase predicted by the model in that region of the phase diagram is a ferromagnetic  $B2$ ,  $B2(F)$ , which develops via a second-order transition. A characteristic feature of this metastable two-phase region is that it ends, with zero width, at a tetracritical point resulting from the intersection of four critical lines: the Curie temperatures of the disordered ( $A2$ ) and ordered ( $B2$ ) structures with the critical lines of order-disorder transitions between the  $A2$  and the  $B2$  phases. We point out that, except for the work of Hasaka<sup>5</sup> that does not include magnetic interactions, the phase diagrams calculated by Sagane and Oki<sup>4</sup> and by Semenovskaya<sup>6</sup> display similar two-phase regions between  $A2(F)$  and  $B2(P)$ . Guided by our findings with the CVM calculations, we recalculated the phase diagram with the same interaction parameters used by Sagane and Oki<sup>4</sup> in both the BW and the CVM approximations. We found that the two-phase region seen in the BW and in the CVM calculations is metastable.

The rest of this paper is organized as follows: In the next section we discuss briefly the CVM and BW models. The results are presented in Sec. III and concluding remarks are given in Sec. IV.

## II. MODEL

In the present thermodynamic model we assume that the energy of the system with  $N$  lattice points is given by

$$E = \frac{N}{2} \sum_{n=1}^2 \omega_n [ V_n (y_{AA}^{(n)} + y_{BB}^{(n)} - 2y_{AB}^{(n)}) - J_n (y_{A_1 A_1}^{(n)} + y_{A_2 A_2}^{(n)} - 2y_{A_1 A_2}^{(n)}) ], \quad (1)$$

where  $\omega_n$ ,  $V_n$ , and  $J_n$  are, respectively, the coordination number, the chemical interaction, and the magnetic interaction for  $n$ th neighbors ( $n=1,2$ ), and where  $y_{ij}^{(n)}$  stands for the probability of finding a  $n$ th-neighbor pair of species  $i$  and  $j$ . In Eq. (1),  $A$  is the magnetic component and  $A_1$  and  $A_2$  represent the two allowed spin configurations. The effective chemical interactions  $V_n$  are given in terms of the atomic interaction  $V_{ij}^{(n)}$  between atomic species  $i$  and  $j$  by  $V_n = (V_{AA}^{(n)} + V_{BB}^{(n)} - 2V_{AB}^{(n)})/4$ .

Positive values of the effective chemical interactions favor pairs of unlike chemical species (ordering), whereas positive magnetic interactions favor alignment of magnetic moments (ferromagnetism). The ground state at  $T=0$

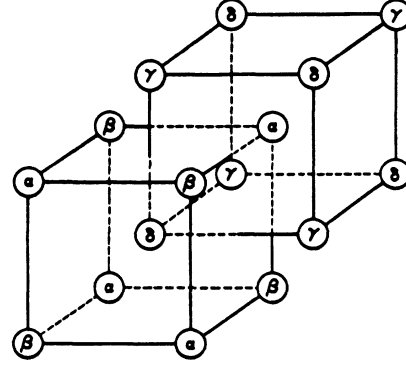


FIG. 1. The four interpenetrating sublattices in the bcc structure.

K structures for the configurational Hamiltonian of Eq. (1) have recently been determined by the authors<sup>9</sup> for all possible values of nearest (NN) and next-nearest neighbors (NNN) chemical and magnetic interactions. In the present work we calculate the equilibrium phase diagram for the set of parameters used by Sagane and Oki<sup>4</sup> to fit the Fe-Al system. In units of the NN chemical interaction ( $V_1 > 0$ ) these are  $V_2 = 0.5V_1$ ,  $J_1 = 0.715V_1$ , and  $J_2 = -0.25V_1$ . For these interaction energies, the chemical ordering at  $T=0$  K is  $DO_3$  for concentrations of the nonmagnetic component  $x_B = 0.25$  and  $x_B = 0.75$ , and  $B2$  for  $x_B = 0.5$ . The magnetic structures of the ground states are ferromagnetic for pure  $A$  (bcc) and for  $DO_3$  at  $x_B = 0.25$ , and antiferromagnetic for the  $B2$  phase and the  $DO_3$  at  $x_B = 0.75$ . The antiferromagnetic ordering is due to the sign of the NNN exchange interaction and to the fact that, at  $T=0$  K, there are no NN magnetic species in either the  $B2$  or the  $DO_3$  ( $x_B = 0.75$ ) phases.

The free energy of the magnetic alloy as a function of temperature and composition was calculated using both the BW and tetrahedron approximation of Kikuchi's<sup>12</sup> CVM. The basic configurational variables in this approximation are the probabilities  $z_{ijkl}$  of finding an irregular tetrahedron, connecting sublattices  $\alpha$ ,  $\beta$ ,  $\gamma$ , and  $\delta$  (see Fig. 1), occupied, respectively, by atomic species  $i$ ,  $j$ ,  $k$ , and  $l$ . In the present case of a binary alloy with one magnetic component, the indices  $i$ ,  $j$ ,  $k$ , and  $l$  can take three values corresponding to atoms  $A_1$ ,  $A_2$ , and  $B$ . The relevant subcluster probabilities, obtained trivially from the  $z_{ijkl}$ , are the single site probability ( $x_i^\gamma$ ), the NN ( $y_{ij}^{\gamma\gamma'}$ ) and NNN ( $u_{ij}^{\gamma\gamma'}$ ) pair probabilities, and the triangle probability  $t_{ijk}^{\gamma\gamma'\gamma''}$ , where roman and greek indices refer to atomic species and sublattices, respectively.

The configurational entropy for a general ordered state is given by

$$S = -Nk \left\{ 6 \sum_{ijkl} L(z_{ijkl}) - 3 \sum_{ijk} [L(t_{ijk}^{\alpha\gamma\beta}) + L(t_{ijk}^{\alpha\delta\beta}) + L(t_{ijk}^{\gamma\alpha\delta}) + L(t_{ijk}^{\gamma\beta\delta})] + \frac{3}{2} \sum_{ij} [L(u_{ij}^{\alpha\beta}) + L(u_{ij}^{\gamma\delta})] + \sum_{ij} [L(y_{ij}^{\alpha\gamma}) + L(y_{ij}^{\alpha\delta}) + L(y_{ij}^{\beta\gamma}) + L(y_{ij}^{\beta\delta})] - \frac{1}{4} \sum_i [L(x_i^\alpha) + L(x_i^\beta) + L(x_i^\gamma) + L(x_i^\delta)] \right\} \quad (2)$$

with  $k$  Boltzmann constant,  $N$  the total number of points in the lattice and where  $L(x) = x \ln(x)$ .

The pair probabilities  $y_{ij}^{(n)}$  in the configurational energy [see Eq. (1)] are given by

$$y_{ij}^{(1)} = (y_{ij}^{\alpha\gamma} + y_{ij}^{\alpha\delta} + y_{ij}^{\beta\gamma} + y_{ij}^{\beta\delta})/4, \quad (3a)$$

$$y_{ij}^{(2)} = (u_{ij}^{\alpha\beta} + u_{ij}^{\gamma\delta})/2. \quad (3b)$$

Combining Eqs. (1) and (2), we obtain the CVM free energy for a general ordered structure which must be minimized with respect to the tetrahedron probabilities. Different minimization algorithms as well as convenient procedures to construct the phase diagram have been discussed extensively in the literature. In order to solve the minimization equations we have used a successive iterations scheme introduced by Kukuchi. Critical lines in the equilibrium phase diagram were obtained by determining the vanishing of the smallest eigenvalue of the  $80 \times 80$  matrix of second derivatives of the free energy, the dimension of which is given by the number of linearly independent tetrahedron variables  $z_{ijkl}$  ( $3^4 - 1$ ). First-order transition lines in the temperature-chemical potential space were obtained from the equality of the grand potentials for different phases.

The free energy function takes a simpler form in the BW approximation. In this case, the configurational entropy is given by

$$S = -Nk \sum_{\nu} \sum_i x_i^{\nu} \ln x_i^{\nu}, \quad (4)$$

where the sums are the four sublattices  $\nu$  and the three species  $i$ . Furthermore, the pair probabilities in Eq. (1) are now approximated by

$$y_{ij}^{(1)} = (x_i^{\alpha} x_j^{\gamma} + x_i^{\alpha} x_j^{\delta} + x_i^{\beta} x_j^{\gamma} + x_i^{\beta} x_j^{\delta})/4, \quad (5a)$$

$$y_{ij}^{(2)} = (x_i^{\alpha} x_j^{\beta} + x_i^{\gamma} x_j^{\delta})/2. \quad (5b)$$

The free energy function is obtained from Eqs. (1), (4), and (5), and the minimization is carried out with respect to the probabilities  $x_i^{\nu}$  at a constant value of the chemical potential. First- and higher-order transition lines were obtained following the same procedure used in the CVM calculations.

The different spatially and magnetically ordered phases described by the present model can be fully characterized using four sublattice magnetizations ( $m_{\nu}$ ), the average concentration of the nonmagnetic component ( $x_B$ ), and three chemical long-range order parameters ( $\eta_n$ ) defined, respectively, by

$$m_{\nu} = x_{A\nu}^{\nu} - x_{A\nu}^{\delta}, \quad (\nu = \alpha, \beta, \gamma, \delta), \quad (6a)$$

$$x_B = (x_B^{\alpha} + x_B^{\beta} + x_B^{\gamma} + x_B^{\delta})/4, \quad (6b)$$

$$\eta_1 = (x_B^{\alpha} + x_B^{\beta} - x_B^{\gamma} - x_B^{\delta})/2, \quad (6c)$$

$$\eta_2 = (x_B^{\alpha} + x_B^{\gamma} - x_B^{\beta} - x_B^{\delta})/2, \quad (6d)$$

$$\eta_3 = (x_B^{\alpha} + x_B^{\delta} - x_B^{\beta} - x_B^{\gamma})/2. \quad (6e)$$

In the paramagnetic state ( $m_{\nu} = 0$  for  $\nu = \alpha, \beta, \gamma$ , and  $\delta$ ), the different types of chemical ordering are given by (i)  $\eta_1 = \eta_2 = \eta_3 = 0$  for the  $A2$  structure, (ii)  $\eta_1 \neq 0$ ,

$\eta_2 = \eta_3 = 0$  for the  $B2$  structure, (iii)  $\eta_2 \neq 0$ ,  $\eta_1 = \eta_3 = 0$  for the  $B32$  structure, and (iv)  $\eta_1 \neq 0$ ,  $\eta_2 = \eta_3 \neq 0$  for the  $DO_3$  structure. We point out that for the set of chemical and magnetic interactions used here, the  $B32$  ordered phase is not stable.

### III. RESULTS

The complete equilibrium phase diagrams calculated using the BW and the tetrahedron approximation of the CVM with NN and NNN interaction energies  $V_1 > 0$ ,  $V_2 = 0.5V_1$ ,  $J_1 = 0.715V_1$ , and  $J_2 = -0.25V_1$  are shown in Figs. 2(a) and 3(a), respectively. We see that the phases found in the two calculations are the same, although there are some notable differences between the two figures: (i) the phase fields in the CVM are much narrower than in the BW approximation, (ii) there is no

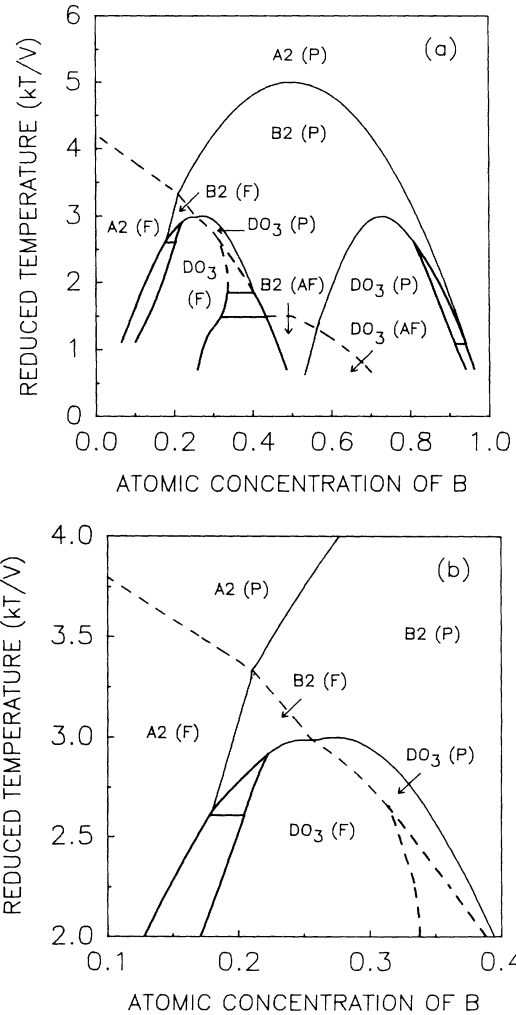


FIG. 2. (a) Temperature-composition phase diagram modeling the Fe-Al system in the Bragg-Williams approximation. Bold and fine lines are used to indicate, respectively, first- and second-order transitions for both chemical (solid line) and magnetic (dashed line) ordering. (b) Detail of the phase diagram. The dotted lines give the metastable two-phase region between the ferromagnetic  $A2$  and paramagnetic  $B2$  phases.

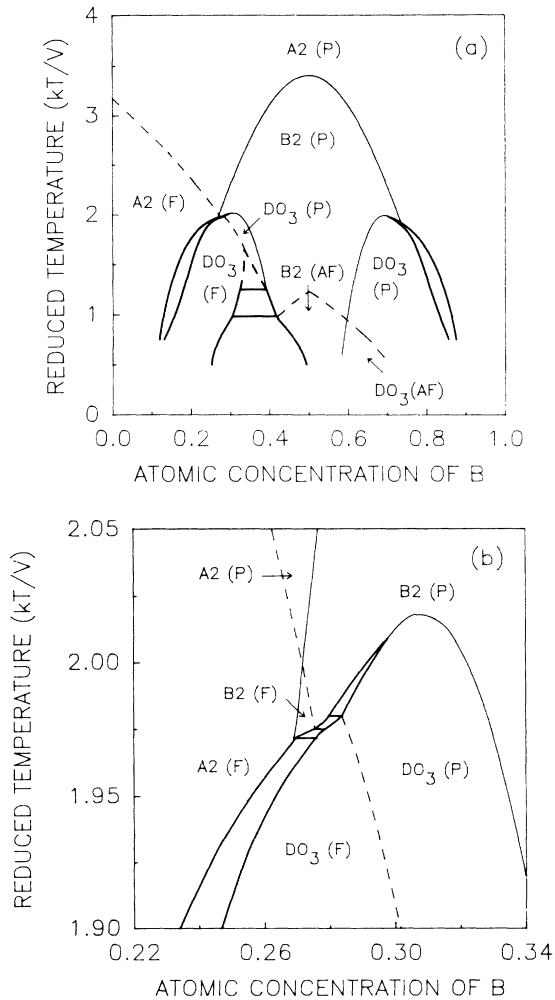


FIG. 3. (a) Temperature-composition phase diagram calculated in the cluster variation approximation using the same interaction parameters of Fig. 2. Bold and fine lines are used to indicate, respectively, first- and second-order transitions for both chemical (solid line) and magnetic (dashed line) ordering. (b) Detail of the phase diagram.

percolation concentration for spatial ordering in the BW approximation, (iii) the second-order line separating the  $B2$  from the  $A2$  phase joins the two-phase region at a higher relative temperature in the CVM than in the BW approximation, (iv) the range of stability of the ferromagnetic  $B2$  is very small in the CVM, and (v) the second-order transition line separating the antiferromagnetic from the paramagnetic  $B2$  phases has a maximum at  $x_B = 0.5$  in the CVM, while this feature is absent in the BW approximation.

Details of the phase diagrams near  $x_B = 0.25$  are shown in Figs. 2(b) and 3(b) for the BW and the CVM approximations, respectively. As pointed out in the Introduction, this region of the phase diagram has attracted considerable theoretical interest. We point out that although there are significant quantitative differences between the results of the BW and the CVM calculations, the general features of the phase diagram are the same in

both approximations. However, we have found qualitative differences between our BW results and those reported by Sagane and Oki<sup>4</sup> using the same interaction parameters. In particular, these authors report the existence of a two-phase region between the ferromagnetic  $A2$  and the paramagnetic  $B2$  phases. Our results indicate that the two-phase region, shown by the dotted lines in Fig. 2(b), is in fact metastable, falling within the region of stability of a ferromagnetic  $B2$ .

#### IV. CONCLUSIONS

Comparison of the CVM and the BW results indicates that the latter are in error by as much as 30%, although the BW approximation appears to reproduce general features of the phase diagram faithfully. We have seen that the bicritical point and, consequently, the two-phase region between the disordered solid solution and the  $B2$  phase cannot be obtained with the values of first- and second-neighbor interactions used by Sagane and Oki.<sup>4</sup> We find that the point in question is a tetracritical point corresponding to the intersection of the Curie temperature of the disordered and ordered phases with the critical lines of order-disordered transitions. As pointed out by Hasaka<sup>5</sup> for nonmagnetic alloys, at least third-nearest-neighbor interactions appear to be necessary in the BW approximation in order to reproduce the tricritical point as well as the  $DO_3$  phase in the phase diagram.

A study of the magnetic transitions by Inden<sup>13</sup> indicates that chemical environmental effects should play an important role in determining the local magnetic moment of Fe in Fe-Al alloys. In general, a reliable description of these environmental effects requires an accurate treatment of chemical short-range order and, consequently, the BW approximation is expected to be inadequate. On the other hand, the CVM provides a sufficiently detailed description of short-range order and its effect on local magnetic moments, as shown recently<sup>14,15</sup> for the cases of Ni-Pt and Co-Pt.

To date, however, CVM theories applied to magnetic<sup>8,9</sup> and nonmagnetic<sup>7,16</sup> bcc alloys include only first- and second-neighbor interactions. Thus, although such theories may accurately describe environmental effects, they will not reproduce the two-phase region and the tricritical point observed in the Fe-Al system. A correct description of this magnetic system will appear to require at least a CVM treatment with up to third-neighbor chemical interactions and many-body magnetic interactions that will simulate the sensitivity of the magnetic moment of Fe to the local chemical environment.

#### ACKNOWLEDGMENTS

This work was partially funded by the National Science Foundation under Grants Nos. DMR-85-10594 and INT-84-09776 and by the Dirección General de Investigación Científica y Superación Académica de la Secretaría de Educación Pública (Mexico) under Grant No. C87-08-0300. One of us (D.A.C.S.) wishes to acknowledge support from Fondo de Apoyo a la Investigación, Universidad Autónoma de San Luis Potosí, Mexico, under Grant No. C87-FAI-10.

- <sup>1</sup>P. R. Swann, W. R. Duff, and R. M. Fisher, *Metall. Trans.* **3**, 409 (1972).
- <sup>2</sup>W. Koster and T. Godecke, *Z. Metallkd.* **71**, 765 (1980).
- <sup>3</sup>R. D. Shull, H. Okamoto, and P. A. Beck, *Solid State Commun.* **20**, 863 (1976).
- <sup>4</sup>H. Sagane and K. Oki, *Trans. Jpn. Inst. Met.* **21**, 811 (1980).
- <sup>5</sup>M. Hasaka, *Trans. Jpn. Inst. Met.* **21**, 660 (1980).
- <sup>6</sup>S. V. Semenovskaya, *Phys. Status Solidi* **B64**, 291 (1974).
- <sup>7</sup>N. S. Golosov, A. M. Tolstik, and L. Ya. Pudan, *J. Phys. Chem. Solids* **37**, 273 (1976).
- <sup>8</sup>B. Dünweg and K. Binder, *Phys. Rev. B* **36**, 6935 (1987).
- <sup>9</sup>D. A. Contreras-Solorio, F. Mejía-Lira, J. L. Morán-López, and J. M. Sanchez, *Phys. Rev. B* **38**, 4955 (1988).
- <sup>10</sup>S. M. Allen and J. W. Cahn, *Acta Metall.* **23**, 1017 (1975).
- <sup>11</sup>S. M. Allen and J. W. Cahn, *Acta Metall.* **24**, 425 (1976).
- <sup>12</sup>R. Kikuchi, *Phys. Rev.* **81**, 988 (1951).
- <sup>13</sup>G. Inden, in *Alloy Phase Diagrams*, edited by L. H. Bennett, T. B. Massalski, and B. C. Giessen (North-Holland, New York, 1983), p. 175.
- <sup>14</sup>C. E. Dahmani, M. C. Cadeville, J. M. Sanchez, and J. L. Morán-López, *Phys. Rev. Lett.* **55**, 1208 (1985).
- <sup>15</sup>M. C. Cadeville and J. L. Morán-López, *Phys. Rep.* **153**, 331 (1987).
- <sup>16</sup>R. Kikuchi and C. M. van Baal, *Scr. Metall.* **8**, 425 (1974).